Electromagnetic scattering I: Scattering dynamics

Joonas Herranen

University of Helsinki

October 5, 2016

Framework for scattering dynamics solution of alignment

1. Background and motivation
2. Integration scheme for rigid body rotations
3. Calculating net torques due to scattering
4. Example results

Dynamics in orientational applications

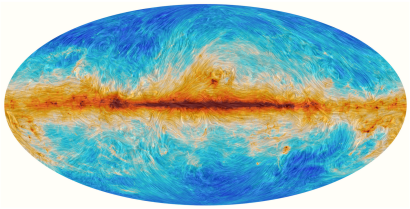

Image: ESA, Planck Collaboration

Image: Terry Miura

- Polarization of interstellar dust particles*
- Optical tweezers**

*Lazarian2008, arXiv: 0901.0146v1
**Ashkin, Science. 1980 Dec 5;210(4474):1081-8

Polarization is due to dust particle alignment

Alignment = Angular momentum J is aligned in space and a principal axis (choose Q_3) aligned with J

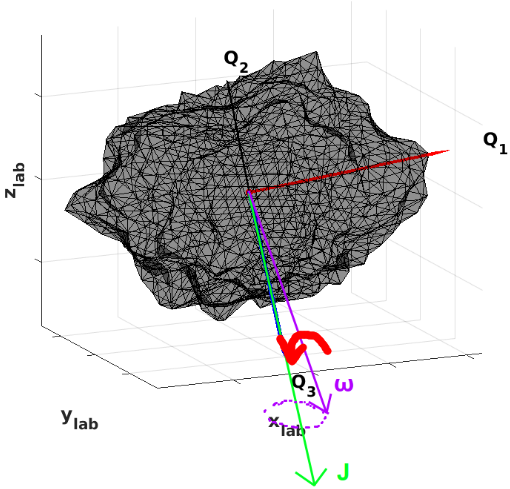

Polarization is due to dust particle alignment

Alignment = Angular momentum J is aligned in space and a principal axis (choose Q_3) aligned with J

- Alignment can be divided to 3 main paradigms
  1. Paramagnetic relaxation
  2. Mechanical alignment
  3. Radiative alignment
- Radiative effects (Lazarian et. al: scattering) has been shown to be relevant most universally

Radiative alignment has been established as central effect

- Alignment is often dominated by scattering, other effects bring out local differences.
- Studies are based on extensive analysis of phase space trajectories.
- The current model of alignment due to scattering is in best agreement with observations.

Table 1 Summary of grain alignment results to date[a]

Observation	Larger grains are better aligned	General alignment only active for $a > 0.045$ µm	H_2 formation enhances alignment	H_2 formation not required for alignment	Alignment seen when $T_{gas} = T_{dust}$	Alignment is not correlated with ferromag-netic inclusions	Alignment is lost at $A_V \sim 20$ mag	Alignment depends on angle between radiation and magnetic fields	Carbon grains are unaligned
Theory									
Davis-Greenstein	−				−				
Super-paramagnetic	+				−	−			
Suprathermal			+	−					
Mechanical			−				−		−
Radiative alignment torque	+	+	+				+	+	+

Andersson et. al. ARAA. 2015;53:501-539

Possible caveat and motivation for explicit integration of dynamics

- Due to techniques used, the analytical model and discrete shapes are somewhat unrealistic and analysis of dynamics require much averaging.
- Our goal is to study the dynamics of more realistically shaped particles based on fundamental electromagnetic interactions.

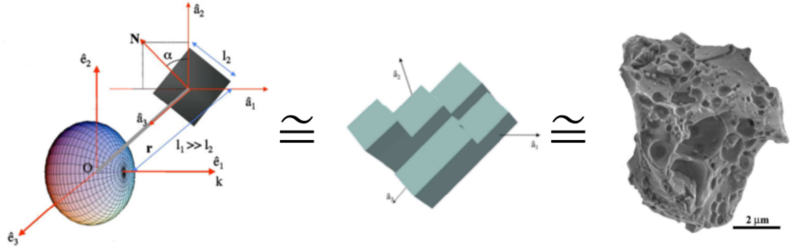

Images: Hoang, Lazarian 2007, 2009

Dynamics of interstellar dust particles - Overview

- Alignment of interstellar dust is complicated, though at heart lies scattering dynamics
- Using integral equation method implementations (both S and V) of Johannes Markkanen, scattering forces and torques can be found rather effortlessly for numerical integration
- Combining above two, an approach based on general equations of motion for rigid body can be formulated to scattering dynamics

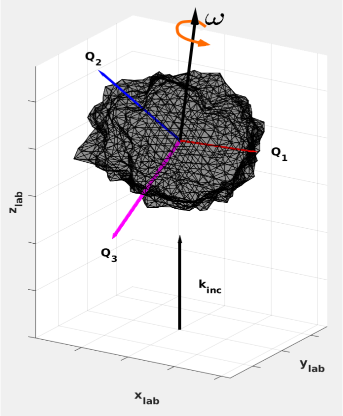

A Gaussian random sphere particle geometry (Muinonen et. al. JQSRT. 1996;55:577-601)

Framework for scattering dynamics solution of alignment

1. Background and motivation
2. Integration scheme for rigid body rotations
3. Calculating net torques due to scattering
4. Example results

Dynamics of rigid bodies

Euler's equations of motion in body frame are

$$\begin{aligned} \vec{\mathsf{N}} &= \mathsf{I}\dot{\vec{\omega}} + \vec{\omega} \times (\mathsf{I}\vec{\omega}), \\ \dot{\mathsf{R}} &= \mathsf{R}\boldsymbol{\Omega}^*. \end{aligned} \tag{1}$$

Rotations are useful to calculate using quaternions Ω[1] and q_R,

$$\dot{q}_\mathsf{R} = \frac{1}{2} q_\mathsf{R} \Omega. \tag{2}$$

[1] matrix representation:

$$\Omega = \begin{pmatrix} 0 & -\omega_x & -\omega_y & -\omega_z \\ \omega_x & & & \\ \omega_y & & \boldsymbol{\Omega}^* & \\ \omega_z & & & \end{pmatrix} = \begin{pmatrix} 0 & -\omega_x & -\omega_y & -\omega_z \\ \omega_x & 0 & -\omega_z & \omega_y \\ \omega_y & \omega_z & 0 & -\omega_x \\ \omega_z & -\omega_y & \omega_x & 0 \end{pmatrix}$$

Numerical solution of Euler's equation

- Two feasible approaches for representing rotations: Matrices and quaternions
- Equation $\vec{\mathrm{N}} = \mathrm{I}\dot{\vec{\omega}} + \vec{\omega} \times (\mathrm{I}\vec{\omega})$ can be solved in matrix form by a Runge-Kutta-4 integrator.
- Other integration schemes are more easily implemented when quaternions are considered
  - Orientation update equation $\dot{q}_{\mathrm{R}} = \frac{1}{2} q_{\mathrm{R}} \Omega$. has trivial integration schemes compared to matrix form $\mathrm{R}(\mathrm{d}t) = \mathrm{I} + \sin \mathrm{d}\phi \, \mathbf{\Omega}^{*}_{\mathrm{avg}} + (1 - \cos \mathrm{d}\phi)(\mathbf{\Omega}^{*}_{\mathrm{avg}})^2$
  - E.g. symplectic (energy conserving) and molecular dynamics (time scale $\sim 10^9$ time steps) integrators are easier to implement.

$\Rightarrow$ Quaternion-based integrator is chosen

Particle geometry determines rotational moment of inertia

Currently, the moment of inertia can be determined from

1. input
2. surface triangle mesh
3. volume tetrahedral mesh
4. spherical fractal aggregates

- Meshing and aggregates allow the simulation of more realistically shaped dust particles

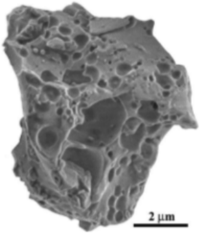

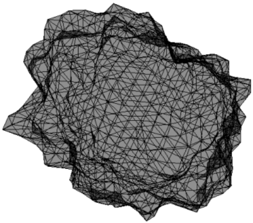

Moment of inertia of a surface mesh

The mass parameters of a triangle mesh are obtained from 10 volume integrals of the form $\int_V p(x,y,z)\,\mathrm{d}V$, with

$$p(x,y,z) \in \{1, x, y, z, x^2, y^2, z^2, xy, xz, yz\}. \tag{3}$$

Finding $\vec{\mathsf{F}}(x,y,z)$, for which $\nabla \cdot \vec{\mathsf{F}}(x,y,z) = p(x,y,z)$, we may apply Stokes' theorem:

$$\begin{aligned}\int_V p(x,y,z)\,\mathrm{d}V = \int_V \nabla \cdot \vec{\mathsf{F}}(x,y,z)\,\mathrm{d}V \\ = \int_S \hat{\mathsf{n}} \cdot \vec{\mathsf{F}}(x,y,z)\,\mathrm{d}S = \sum_{f \in S} \int_f \hat{\mathsf{n}}_f \cdot \vec{\mathsf{F}}(x,y,z)\,\mathrm{d}S.\end{aligned} \tag{4}$$

We are left with 10 surface integrals $(\hat{\mathsf{n}}_f \cdot \hat{\mathsf{e}}_i) \int_f q(x,y,z)\,\mathrm{d}S$, with $q(x,y,z) \in \{x, x^2, y^2, z^2, x^3, y^3, z^3, x^2y, xz^2, y^2z\}$.

Moment of inertia of a surface mesh

Parametrize triangle face i with vertices $\vec{\mathsf{P}}_i = (x_i, y_i, z_i)$, $i = 0, 1, 2$ and edges $\vec{\mathsf{E}}_j = \vec{\mathsf{P}}_j - \vec{\mathsf{P}}_0 = (\alpha_j, \beta_j, \gamma_j)$, $j = 1, 2$, as

$$\begin{aligned} \vec{\mathsf{P}}(u, v) &= \vec{\mathsf{P}}_0 + u\vec{\mathsf{E}}_1 + v\vec{\mathsf{E}}_2 \\ &= (x_0 + \alpha_1 u + \alpha_2 v, y_0 + \beta_1 u + \beta_2 v, z_0 + \gamma_1 u + \gamma_2 v) \\ &= (x(u, v), y(u, v), z(u, v)),\ u \geq 0,\ v \geq 0,\ u + v \leq 1. \end{aligned} \tag{5}$$

Now

$$\mathrm{d}S = \left| \frac{\partial \vec{\mathsf{P}}}{\partial u} \times \frac{\partial \vec{\mathsf{P}}}{\partial v} \right| \mathrm{d}u\mathrm{d}v = \left| \vec{\mathsf{E}}_1 \times \vec{\mathsf{E}}_2 \right| \mathrm{d}u\mathrm{d}v, \tag{6}$$

and

$$\begin{aligned} \hat{\mathsf{n}}_f &= \frac{\vec{\mathsf{E}}_1 \times \vec{\mathsf{E}}_2}{\left|\vec{\mathsf{E}}_1 \times \vec{\mathsf{E}}_2\right|} = \frac{(\beta_1\gamma_2 - \beta_2\gamma_1, \alpha_2\gamma_1 - \alpha_1\gamma_2, \alpha_1\beta_2 - \alpha_2\beta_1)}{\left|\vec{\mathsf{E}}_1 \times \vec{\mathsf{E}}_2\right|} \\ &= \frac{(\delta_0, \delta_1, \delta_2)}{\left|\vec{\mathsf{E}}_1 \times \vec{\mathsf{E}}_2\right|}. \end{aligned} \tag{7}$$

Moment of inertia of a surface mesh

We now have parametrized all integrals as

$$\begin{aligned}&(\hat{n}_f \cdot \hat{e}_i) \int_f q(x,y,z)\,\mathrm{d}S \\ &= (\vec{E}_1 \times \vec{E}_2 \cdot \vec{e}_i) \int_0^1 \int_0^{1-v} q(x(u,v), y(u,v), z(u,v))\,\mathrm{d}u\mathrm{d}v,\end{aligned} \tag{8}$$

explicitly

$$\begin{aligned}
(\hat{n}_f \cdot \hat{\imath}) \int_f x\,\mathrm{d}S &= \frac{\delta_0}{6} f_1(x), & (\hat{n}_f \cdot \hat{\jmath}) \int_f y^3\,\mathrm{d}S &= \frac{\delta_1}{20} f_3(y),\\
(\hat{n}_f \cdot \hat{\imath}) \int_f x^2\,\mathrm{d}S &= \frac{\delta_0}{12} f_2(x), & (\hat{n}_f \cdot \hat{k}) \int_f z^3\,\mathrm{d}S &= \frac{\delta_2}{20} f_3(z),\\
(\hat{n}_f \cdot \hat{\jmath}) \int_f y^2\,\mathrm{d}S &= \frac{\delta_0}{12} f_2(y), & (\hat{n}_f \cdot \hat{\imath}) \int_f x^2 y\,\mathrm{d}S &= \frac{\delta_0}{60} (y_0 g_0(x) + y_1 g_1(x) + y_2 g_2(x)),\\
(\hat{n}_f \cdot \hat{k}) \int_f z^2\,\mathrm{d}S &= \frac{\delta_0}{12} f_2(z), & (\hat{n}_f \cdot \hat{\jmath}) \int_f y^2 z\,\mathrm{d}S &= \frac{\delta_1}{60} (z_0 g_0(y) + z_1 g_1(y + z_2 g_2(y)),\\
(\hat{n}_f \cdot \hat{\imath}) \int_f x^3\,\mathrm{d}S &= \frac{\delta_0}{20} f_3(x), & (\hat{n}_f \cdot \hat{k}) \int_f z^2 x\,\mathrm{d}S &= \frac{\delta_2}{60} (x_0 g_0(z) + x_1 g_1(z) + x_2 g_2(z)).
\end{aligned} \tag{9}$$

$$\begin{aligned}
f_1(w) &= a + w_2, & f_2(w) &= c + w_2 f_1(w),\\
f_3(w) &= w_0 b + w_1 c + w_2 f_2(w), & g_i(w) &= f_2(w) + w_i(f_1(w) + w_i),\\
w &= x, y, \text{ or } z, & a &= w_0 + w_1, b = w_0^2,\ c = b + w_1 a
\end{aligned} \tag{10}$$

Moment of inertia of a volume mesh

Using tetrahedral parametrization similar to that of FEM, the volume integrals will have the form

$$\int_D f(x, y, z)\,\mathrm{d}V$$
$$= |\det(J)| \int_0^1 \mathrm{d}\xi \int_0^{1-\xi} \mathrm{d}\eta \int_0^{1-\xi-\eta} \mathrm{d}\zeta \; f\left[x(\xi,\eta,\zeta), y(\xi,\eta,\zeta), z(\xi,\eta,\zeta)\right] \quad (11)$$

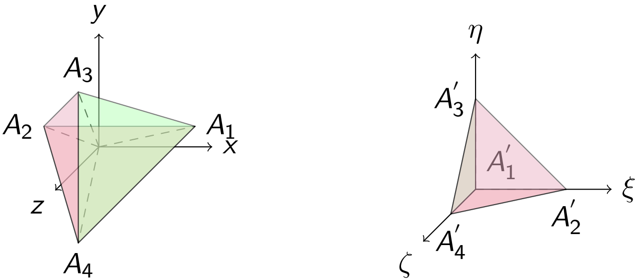

Figure: Arbitrary and parametrized tetrahedrons

Moment of inertia of a volume mesh

The moment of inertia tensor of a single tetrahedron at point Q has components

$$\mathsf{I}_Q = \begin{pmatrix} \int (y^2 + z^2)\mathrm{d}m & -\int xy\mathrm{d}m & -\int xz\mathrm{d}m \\ -\int xy\mathrm{d}m & \int (x^2 + z^2)\mathrm{d}m & -\int yz\mathrm{d}m \\ -\int xz\mathrm{d}m & -\int yz\mathrm{d}m & \int (x^2 + y^2)\mathrm{d}m \end{pmatrix}, \quad (12)$$

which can be translated to the center of mass by the parallel axis theorem,

$$\mathsf{J} = \mathsf{I} + m[(r \cdot r)1_3 - r \otimes r], \quad (13)$$

where 1_3 is a unit matrix and $\otimes$ the outer product.

"Validation" of integrator with intermediate axis theorem

Choose geometry with three distinct principal moment of inertia and initial $\boldsymbol{\omega} = (\lambda, \omega_2, \mu)$ in principal axis frame. It can be shown the time evolution of the perturbation in *torque-free* rotation λ is

$$\ddot{\lambda} - \left[\frac{(I_2 - I_1)(I_3 - I_2)}{I_1 I_3}\right] \omega_2^2 \lambda = 0. \tag{14}$$

The solutions to (14) are of form $\lambda = Ae^{kt} + Be^{-kt}$: exponential divergence from initial state.

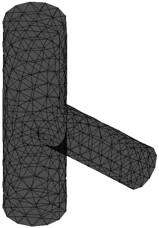

Example geometry with 3 distinct principal moments of inertia

Unstable, torque-free T-handle rotation

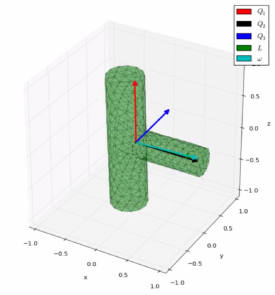

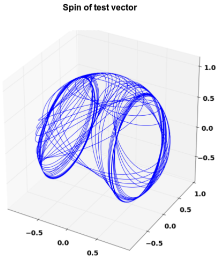

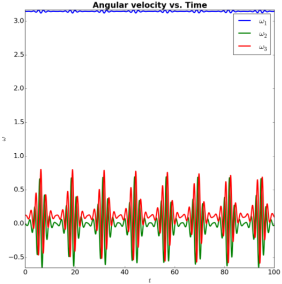

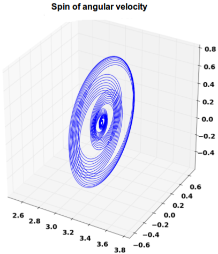

Stable, torque-free T-handle rotation

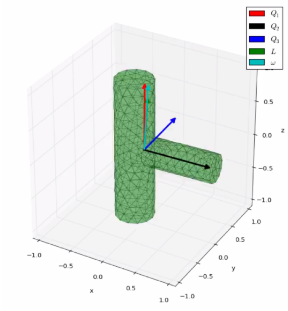

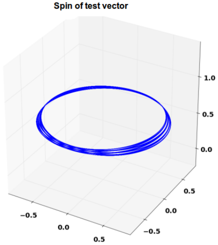

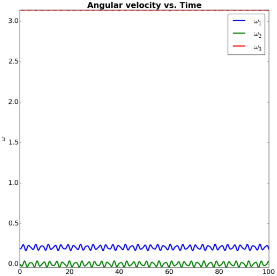

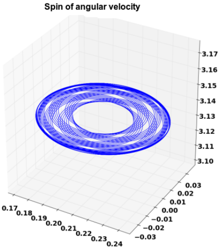

Framework for scattering dynamics solution of alignment

1. Background and motivation
2. Integration scheme for rigid body rotations
3. Calculating net torques due to scattering
4. Example results

The idea behind an integral equation method

Equivalent currents, which induce the scattered fields, replace the actual scatterer and the total field can be represented as a sum of the incident field and the scattered field, which is written in terms of the equivalent currents (example below: equivalent surface currents).

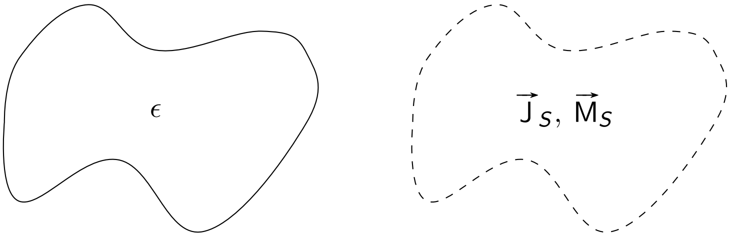

Choice of boundary conditions and discretization scheme result in a matrix equation, from which the total fields are numerically obtained

Example: Derivation of the Stratton-Chu equations

Consider a time-harmonic problem with symmetrized Maxwell equations

$$\nabla \times \vec{E} = i\omega\mu\vec{H} - \vec{M}, \qquad \nabla \cdot \vec{E} = \frac{\rho}{\varepsilon},$$
$$\nabla \times \vec{H} = -i\omega\varepsilon\vec{E} + \vec{J}, \qquad \nabla \cdot \vec{H} = \frac{m}{\mu}, \tag{15}$$

continuity equations

$$\nabla \cdot \vec{J} = i\omega\rho, \qquad \nabla \cdot \vec{M} = i\omega m, \tag{16}$$

and the vector wace equations of a linear, homogeneous and isotropic medium

$$\nabla \times \nabla \times \vec{E} - k^2\vec{E} = i\omega\mu\vec{J} - \nabla \times \vec{M},$$
$$\nabla \times \nabla \times \vec{H} - k^2\vec{H} = i\omega\varepsilon\vec{M} + \nabla \times \vec{J}. \tag{17}$$

Example: Derivation of the Stratton-Chu equations

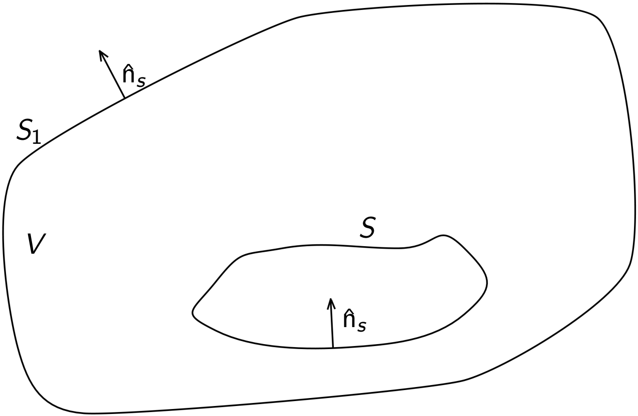

Scattering problem in volume V with boundary S_1, containing dielectric objects with boundary S. Note the choice of normal vector directions.

Example: Derivation of the Stratton-Chu equations

The goal is to write the total fields $\vec{E}$ ja $\vec{H}$ in terms of the current densities $\vec{J}$ ja $\vec{M}$. Starting with the vector Green's theorem

$$\int_V (\vec{Q}\cdot\nabla\times\nabla\times\vec{P}-\vec{P}\cdot\nabla\times\nabla\times\vec{Q})\,\mathrm{d}V = \int_\Sigma (\vec{P}\times\nabla\times\vec{Q}-\vec{Q}\times\nabla\times\vec{P})\cdot\mathrm{d}\vec{S}, \tag{18}$$

the problem is solved similarly as with static fields and the scalar Green's theorem.

Example: Derivation of the Stratton-Chu equations

Choosing $\vec{\mathsf{P}} = \vec{\mathsf{E}}$ and $\vec{\mathsf{Q}} = \phi\hat{\mathsf{a}}$, where $\phi = \frac{e^{\mathrm{i}kr}}{r}$, $r = |\vec{\mathsf{x}} - \vec{\mathsf{x}}'|$ has the form of the Helmholtz Green's function, and $\hat{\mathsf{a}}$ is an arbitrary unit vector, extensive manipulation will result in a surface integral form

$$\begin{aligned} &\int_V \mathrm{i}\omega\mu\phi\vec{\mathsf{J}} + \nabla\phi \times \vec{\mathsf{M}} + \frac{\rho}{\varepsilon}\nabla\phi \,\mathrm{d}V \\ &= \int_\Sigma (\hat{\mathsf{n}} \times \vec{\mathsf{E}}) \times \nabla\phi + (\hat{\mathsf{n}} \cdot \vec{\mathsf{E}})\nabla\phi + \mathrm{i}\omega\mu(\hat{\mathsf{n}} \times \vec{\mathsf{H}})\phi \,\mathrm{d}S. \end{aligned} \tag{19}$$

Example: Derivation of the Stratton-Chu equations

Choosing $\vec{P} = \vec{E}$ and $\vec{Q} = \phi\hat{a}$, where $\phi = \frac{e^{ikr}}{r}$, $r = |\vec{x} - \vec{x}'|$ has the form of the Helmholtz Green's function, and $\hat{a}$ is an arbitrary unit vector, extensive manipulation will result in a surface integral form

$$\begin{aligned} &\int_V i\omega\mu\phi\vec{J} + \nabla\phi \times \vec{M} + \frac{\rho}{\varepsilon}\nabla\phi \, dV \\ &= \int_\Sigma (\hat{n} \times \vec{E}) \times \nabla\phi + (\hat{n} \cdot \vec{E})\nabla\phi + i\omega\mu(\hat{n} \times \vec{H})\phi \, dS. \end{aligned} \tag{20}$$

All differentiability and boundary conditions for both $\vec{E}$ and $\vec{Q}$, as well as the singularity of ϕ at $\vec{x} = \vec{x}'$ must still be extracted from this solution.

Example: Derivation of the Stratton-Chu equations

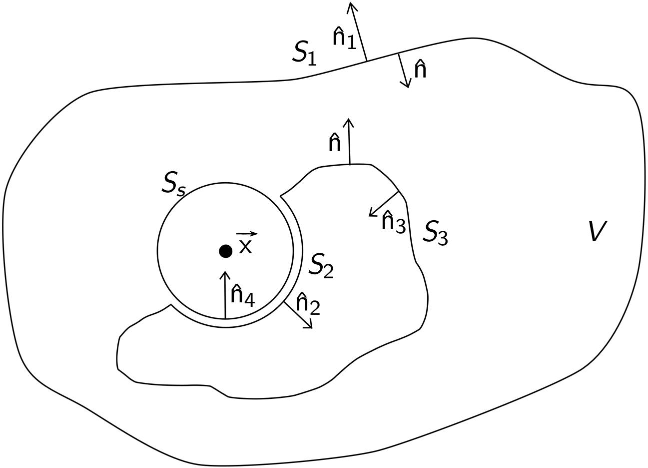

Figure: The case where the observation point lies on the scattering surface. Deforming the surface and isolating the point with a spherical surface, the problem is solved in the limit $S_s \to 0$

Example: Derivation of the Stratton-Chu equations

A thorough treatment of other discontinuities can be found e.g. in (Volakis and Sertel. Integral Equation Methods for Electromagnetics. Scitech Publishing, 2012.). Resulting integral equations for the total fields are

$$\vec{\mathrm{E}}(\vec{\mathrm{x}}) = \frac{T(\vec{\mathrm{x}})}{4\pi}\int_V \mathrm{i}\omega\mu\phi\vec{\mathrm{J}} + \nabla'\phi\times\vec{\mathrm{M}} + \frac{\rho}{\varepsilon}\nabla'\phi\,\mathrm{d}V'$$
$$- \frac{T(\vec{\mathrm{x}})}{4\pi}\fint_{S_1+S}(\hat{\mathrm{n}}'\times\vec{\mathrm{E}})\times\nabla'\phi + (\hat{\mathrm{n}}'\cdot\vec{\mathrm{E}})\nabla'\phi + \mathrm{i}\omega\mu(\hat{\mathrm{n}}'\times\vec{\mathrm{H}})\phi\,\mathrm{d}S', \tag{21}$$

$$\vec{\mathrm{H}}(\vec{\mathrm{x}}) = \frac{T(\vec{\mathrm{x}})}{4\pi}\int_V \mathrm{i}\omega\varepsilon\phi\vec{\mathrm{M}} + \vec{\mathrm{J}}\times\nabla'\phi + \frac{m}{\mu}\nabla'\phi\,\mathrm{d}V'$$
$$- \frac{T(\vec{\mathrm{x}})}{4\pi}\fint_{S_1+S}(\hat{\mathrm{n}}'\times\vec{\mathrm{H}})\times\nabla'\phi + (\hat{\mathrm{n}}'\cdot\vec{\mathrm{H}})\nabla'\phi - \mathrm{i}\omega\varepsilon(\hat{\mathrm{n}}'\times\vec{\mathrm{E}})\phi\,\mathrm{d}S', \tag{22}$$

where $T(\vec{\mathrm{x}}) = (1-\Omega/4\pi)^{-1}$ and $\fint_{S_1+S}$ is the principal value integral over S_1 and S.

The Maxwell stress tensor

Maxwell stress tensor T represents the interaction between the electromagnetic forces and mechanical momentum,

$$\mathsf{T}_{ij} = \varepsilon_0 \left(E_i E_j - \frac{1}{2}\delta_{ij} E^2 \right) + \frac{1}{\mu_0} \left(B_i B_j - \frac{1}{2}\delta_{ij} B^2 \right). \qquad (23)$$

If the EM fields can be determined anywhere near the surface of the particle, then the Maxwell stress tensor can be determined using sample points at the surface.

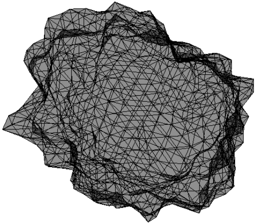

EM-forces given by known Maxwell stress tensor, T

Lorentz force density in terms of T is

$$\vec{f} = \nabla \cdot \mathsf{T} - \varepsilon_0 \mu_0 \frac{\partial \vec{S}}{\partial t} = \nabla \cdot \mathsf{T} \cancel{- \varepsilon_0 \mu_0 \frac{\partial \vec{S}}{\partial t}} \text{ (averaged)}, \tag{24}$$

which gives total force and torque as functions of the total fields,

$$\begin{aligned} \vec{F} &= \oint_S \mathsf{T} \cdot \hat{n} \, \mathrm{d}S, \\ \vec{N} &= \oint_S \vec{r} \times (\mathsf{T} \cdot \hat{n}) \, \mathrm{d}S. \end{aligned} \tag{25}$$

$\Rightarrow$ Liftoff! We have a liftoff...

Framework for scattering dynamics solution of alignment

1. Background and motivation
2. Integration scheme for rigid body rotations
3. Calculating net torques due to scattering
4. Example results

Primary field from starlight (blackbody radiation)

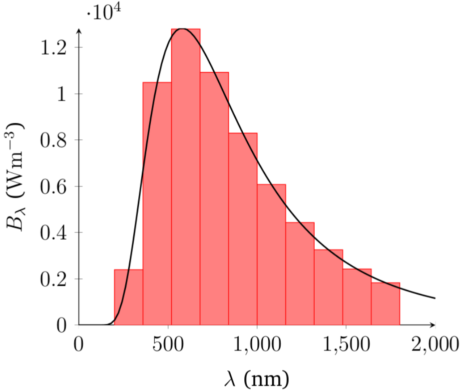

- Spectral radiance Maxwell distributed
- Discretization over wavelength band 200 – 2000 nm

$$B_\lambda(T) = \frac{2hc^2}{\lambda^5}\frac{1}{e^{hc/\lambda kT} - 1}, \; [B_\lambda] = \mathrm{Wm}^{-3}\mathrm{sterad}^{-1}. \qquad (26)$$

Primary field from starlight (blackbody radiation)

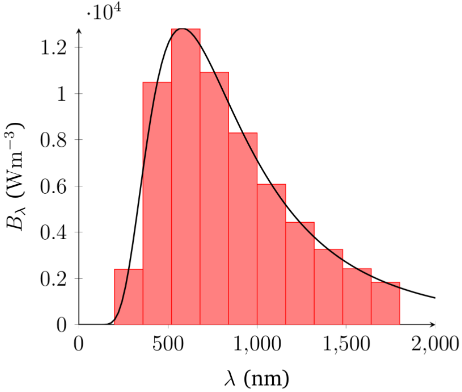

- Poynting theorem relates total intensity and the time-averaged E-field amplitude
- Normalizing the peak intensity to unity we have discretized blackbody amplitudes

$$|E|_{\lambda_i} = \left(\frac{B_{\lambda_i}(T)}{N_{B_{\lambda_i}}(T)} \right)^{\frac{1}{2}} |E|_{\max}, \; N_{B_\lambda}(T) = \frac{2hc^2}{b^5} \frac{T^5}{e^{hc/bk} - 1}. \quad (27)$$

Simulation of rotation in blackbody radiation

Test geometry ($\epsilon = 3.0 + 0.1i$, $a = 10^{-7}$ m), $\rho = 2000$ kg/m^3 at $\sim 10^4$ AU from a star ($T_{bb} = 4600$ K)

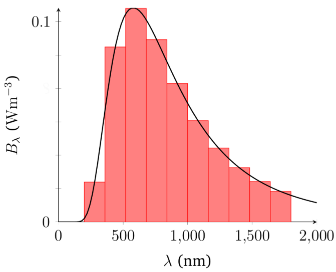

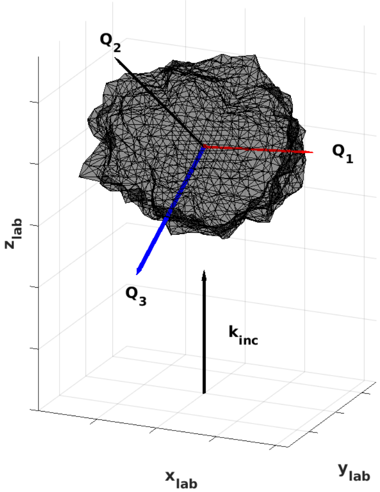

Particle with $I_p = (5.64, 7.81, 8.57) \cdot 10^{-33}\,\mathrm{kgm}^2$

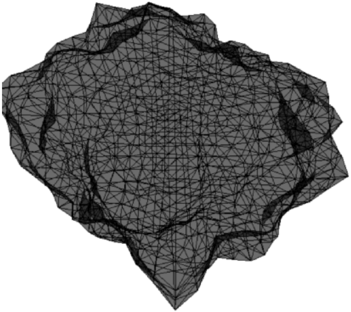

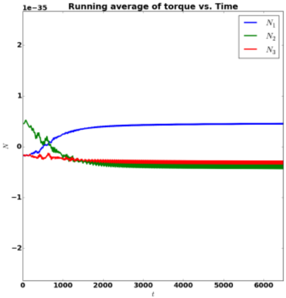

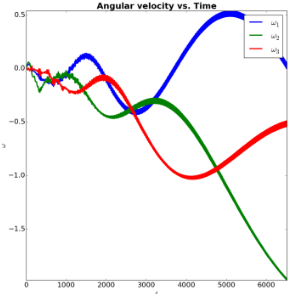

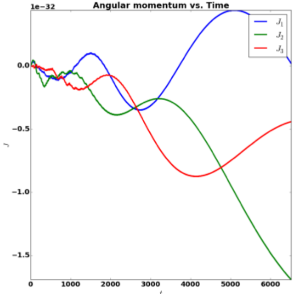

Particle with $I_p = (5.64, 7.81, 8.57) \cdot 10^{-33}\,\mathrm{kgm}^2$

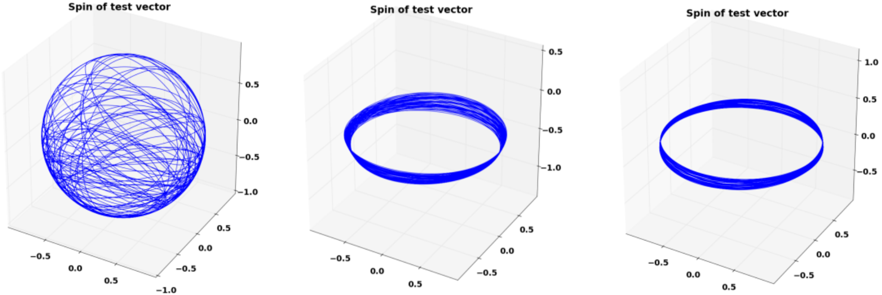

Spinning states of the particle at 0-5 min, 50-55 min and 95-100 min, respectively

Particle with $I_p = (1.29, 1.44, 1.53) \cdot 10^{-33}\,\mathrm{kgm}^2$

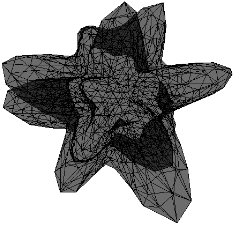

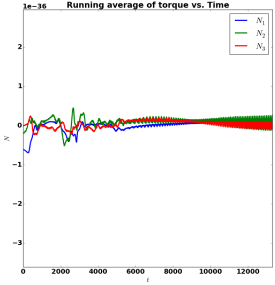

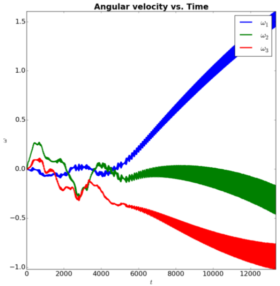

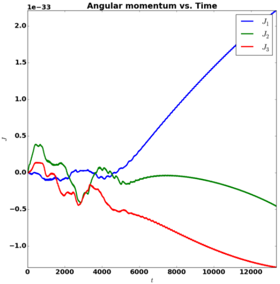

Particle with $I_p = (1.29, 1.44, 1.53) \cdot 10^{-33}\,\mathrm{kgm}^2$

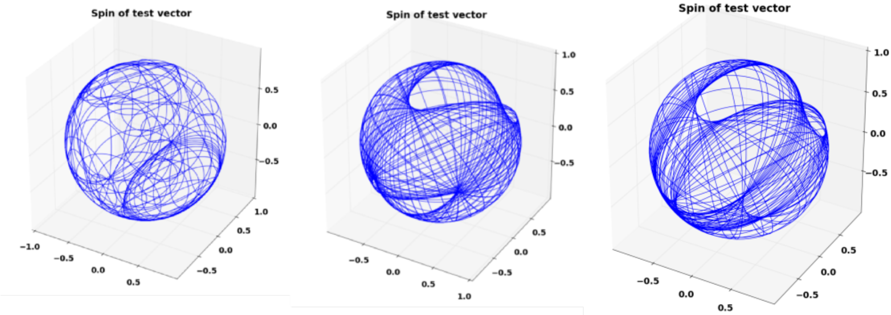

Spinning states of the particle at 0-5 min, 105-110 min and 225-230 min, respectively